CHEMISTRY
A EUROPEAN JOURNAL

DOI: 10.1002/chem.200903067

Switchable Cucurbituril–Bipyridine Beacons

Mantosh K. Sinha,[a] Ofer Reany,[a] Galit Parvari,[a] Ananta Karmakar,[a] and Ehud Keinan*[a, b]

Abstract: 4-Aminobipyridine derivatives form strong inclusion complexes with cucurbit[6]uril, exhibiting remarkably large enhancements in fluorescence intensity and quantum yields. The remarkable complexation-induced pK_a shift ($\Delta pK_a = 3.3$) highlights the strong charge–dipole interaction upon binding. The reversible binding phenomenon can be used for the design of switchable beacons that can be incorporated into cascades of binding networks. This concept is demonstrated herein by three different applications: 1) a switchable fluorescent beacon for chemical sensing of transition metals and other ligands; 2) direct measurement of binding constants between cucurbit[6]uril and various nonfluorescent guest molecules; and 3) quantitative monitoring of biocatalytic reactions and determination of their kinetic parameters. The latter application is illustrated by the hydrolysis of an amide catalyzed by penicillin G acylase and by the elimination reaction of a β-cabamoyloxy ketone catalyzed by aldolase antibody 38C2.

Keywords: biocatalysis · cucurbiturils · fluorescence · inclusion compounds · sensors

Introduction

Biological systems are characterized by complex, interconnected networks of noncovalent binding equilibria in which one binding event triggers a cascade of other binding phenomena. These equilibria cascades can finally give rise to a specific functional output, such as the folding of proteins and RNA.[1] This concept can be applied also to nonbiological systems for the construction of specific chemical sensors. Of particular interest are sensors that are based on host–guest chemistry because they can be designed to be specific, selective, and highly sensitive.

Aiming at the construction of a network of interconnected binding events, we focused our attention on the cucurbiturils[2] as preferred host molecules because their unique binding properties and rigid structure,[3] which includes two highly polar portals and a hydrophobic interior, could be harnessed for altering the photophysical properties of various guest molecules.[4] It has been demonstrated that cucurbit[7]uril (CB[7]) can encapsulate various fluorescent dye molecules and thereby modify their UV/Vis absorption spectra, fluorescence intensities, and pK_a values.[5]

While searching for guest molecules that could participate in other binding events, we were attracted by the 2,2′-bipyridine derivatives due to their fluorescence properties and independent ability to form stable complexes with essentially any transition metal. It has been recently reported that 5,5′-dimethyl-2,2′-bipyridine binds to either tetramethyl- or dicyclohexyl-CB[6] (CB[6] = cucurbit[6]uril), but that binding event did not lead to fluorescence enhancement.[6] On the contrary, the formation of 1:1 host–guest complexes between those molecules resulted in fluorescence quenching. This phenomenon probably reflects a binding mode in which only one of the two pyridine rings is included within the cucurbituril cavity whereas the second ring remains exposed to the solvent and rotates freely around the C–C single bond, thus populating many stable conformations. This binding mode, particularly with 5,5′-dimethyl-2,2′-bipyridine and tetramethyl-CB[6], was predicted by quantum mechanical calculations and confirmed by single-crystal X-ray crystallography.[6a]

[a] M. K. Sinha, Dr. O. Reany, G. Parvari, Dr. A. Karmakar, Prof. E. Keinan
Schulich Faculty of Chemistry
Technion—Israel Institute of Technology
Technion City, Haifa 32000 (Israel)
Fax: (+972) 48293913
E-mail: keinan@technion.ac.il

[b] Prof. E. Keinan
Department of Molecular Biology and
the Skaggs Institute for Chemical Biology
The Scripps Research Institute
10550 North Torrey Pines Road
La Jolla, California 92037 (USA)

Supporting information for this article is available on the WWW under http://dx.doi.org/10.1002/chem.200903067.

We assumed that this situation could be drastically changed if the bipyridine guest were forced to reside completely within the cavity of CB[6] (**1**). We anticipated that this goal could be achieved by substituting position 4 of the bipyridine molecule with an amine group to allow for a double interaction of the guest molecule with both portals of the CB host. We also expected that **1**, being the smallest practical host in the cucurbituril family, could induce significant changes in the photophysical properties of the guest molecule by imposing maximal restriction on its conformational freedom. In this respect, host **1** seems to have advantages over CB[7], which has been extensively used by Nau for substrate-selective supramolecular assays.[1b,7]

Herein we report 4-aminobipyridine derivatives, such as **2**, **3**, **4**, and **5**, which exhibit remarkably large enhancements in fluorescence intensity and quantum yields upon formation of inclusion complexes with **1**. We also report that this enhanced fluorescence phenomenon can be utilized for the design of switchable beacons that can be incorporated within cascades of binding networks. In addition, we show that the beacon fluorescence intensity can be harnessed for chemical sensing, for direct measurement of binding constants between **1** and various nonfluorescent guest molecules (**6**, **7**, and **8**), and for quantitative monitoring of biocatalytic reactions and determination of their kinetic parameters.

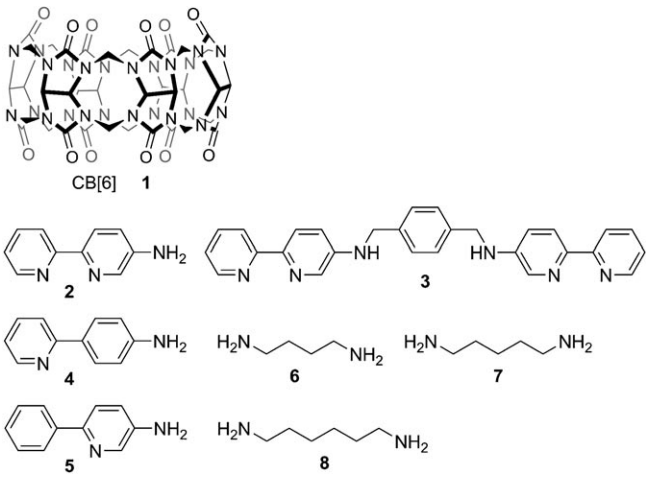

Abstract in Hebrew:

אבוקה ממותגת על בסיס אמינופירידין וקיוקורביטוריל

קומפלקסים יציבים מאד מסוג אורח-מארח נוצרים בתמיסה משותפת של קיוקורביטו[6]ריל, אשר משמש כמארח, ונגזרות של 4-אמינופירידין. נמצא כי לקומפלקסים אלו תכונות ספקטרליות יוצאות דופן, כגון עוצמת פלואורסצנציה בלתי רגילה וניצולות קוונטיות כמותיות. בנוסף לכך, יצירת הקומפלקס גורמת להיסטים גדולים מאד של חומציות האורח (ΔpK_a = 3.3), תופעה אשר נובעת מכוחות משיכה חזקים בין המטען החיובי של האורח והדיפול הגדול של המארח. את התופעות הללו, אשר נובעות מתהליך הקישור ההפיך, ניתן לנצל למספר שימושים, בעיקר לצורך בניה של אבוקות ממותגות, שאותן ניתן לשלב ברשתות מורכבות של מערכות שווי משקל. בעבודה הנוכחית מודגם העקרון הזה באמצעות שלושה יישומים שונים: (א) אבוקה ממותגת לצרכים של חישה כימית של מתכות המעבר ושל ליגנדות שונות, (ב) מדידה ישירה של קבועי קישור בין קיוקורביטוריל לבין מולקולות אורח בלתי פלואורסצנטיות, (ג) ניטור כמותי של תגובות ביוקטליטיות וקביעת הפרמטרים הקינטיים שלהם. היישום השלישי מודגם על ידי תגובת הידרוליזה של קשר אמידי בקטליזה של האנזים פניצילין G, ותגובת בטה-אלימינציה של בטה-קרבמואילוקסי-קטון בקטליזה של נוגדן אלדולאז, 38C2.

Results and Discussion

Compounds **2**, **3**, and **5** were prepared from 2-bromo-5-aminopyridine (**9**), and compound **4** was prepared from 4-iodoaniline (**10**; Scheme 1). Thus, protection of the amine group in **9** in the form of a 1,5-dimethylpyrrole derivative (**11**) was followed by a Stille cross coupling with 2-(tributyltin)pyridine and a palladium(0) catalyst to give protected bipyridine **13**. Deprotection of the amine group by using aqueous hydroxylamine gave 4-amino-2,2′-bipyridine **2** in 67% overall yield. By starting with **10** and using the same sequence of reactions, 4-(2-pyridyl)aniline (**4**) was obtained in a similarly high overall yield. Compound **5** was obtained from **9** by first converting it to the bis-Boc derivative (**15**) and then performing a Suzuki coupling with phenylboronic acid by using Fu's palladium catalyst.[8] Finally, deprotection of the amine group gave **5** in 60% overall yield. Monoprotection of **9** with only one Boc group to give **17** followed by double alkylation with 1,4-bis(bromomethyl)benzene under basic conditions gave **18**. The latter underwent the above-mentioned Stille coupling to give **19**, which, upon deprotection under acidic conditions, afforded **3**.

The absorption spectra of **2** and **2@1** were found to be quite similar, with the latter being redshifted by 15 to 18 nm (Figure 1 and Table 1, and Figure S1 in the Supporting Information). These spectra are dominated by an intense π–π* transition of the protonated (low-energy band) and the neutral (high-energy band) bipyridine ligands.[9] Protonation of **2** is associated with a nine-fold intensity enhancement in the low-energy band and a two-fold intensity decrease in the high-energy band. The analogous effects in the spectrum intensities of **2@1** are a five-fold enhancement and a two-fold decrease, respectively. The spectral changes of **2** exhibit two

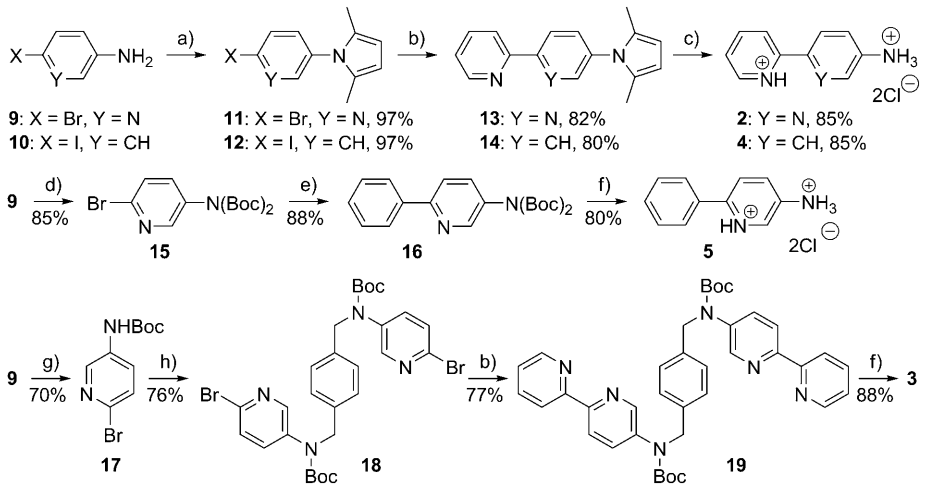

Scheme 1. Synthesis of guest molecules **2**–**5**. Reagents and conditions: a) hexane-2,5-dione, *p*-TsOH (cat.), toluene, reflux, 4 h; b) 2-(tributyltin)pyridine, $[Pd(PPh_3)_4]$, toluene, 130 °C, 24 h; c) $NH_2OH{\cdot}HCl$, Et_3N, EtOH/H_2O, 100 °C, 24 h; d) $(Boc)_2O$, Et_3N, 4-dimethylaminopyridine (DMAP), CH_2C_2, RT, 48 h; e) $PhB(OH)_2$, $CsCO_3$, dioxane, $Pd(tBu_3P)_2$ (5 mol %), 80 °C, 16 h; f) 4 N HCl, EtOH, RT, 16 h; g) $(Boc)_2O$, Et_3N, CH_2Cl_2, RT, 12 h; h) 1,4-bis(bromomethyl)benzene, NaH, *N*,*N*-dimethylformamide (DMF), RT, 24 h; f) 4 N HCl, EtOH, RT, 16 h.

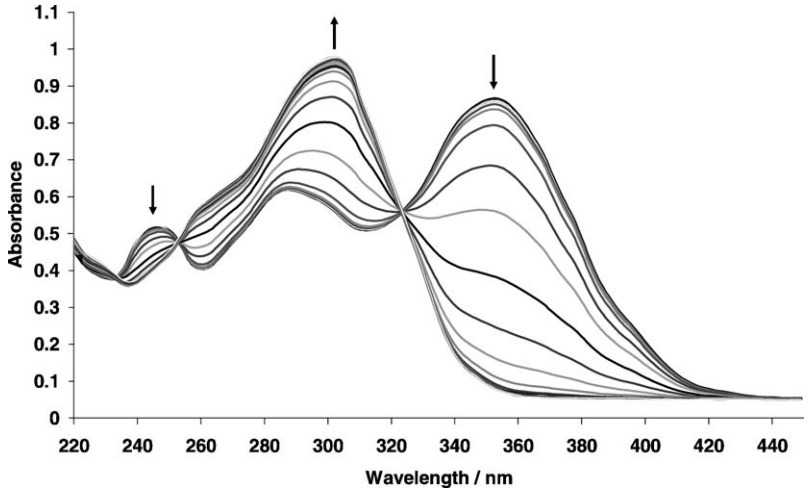

Figure 1. Changes in the UV/Vis spectrum of **2** as a function of pH (3–11) at 298 K.

isosbestic points at $\lambda = 323$ and 254 nm, which allow for determination of the two pK_a values (Scheme 2). The first pK_a value of 4.77 was determined by monitoring the intensity changes at $\lambda = 302$ and 353 nm, which characterize the bipyridine part of the molecule (Scheme 2 and Figure 2, right),[9] whereas the second pK_a value of 5.04, which is associated with the amine group, was determined by monitoring the changes at $\lambda = 245$ and 260 nm (Figure 2, left). A second protonation of the bipyridine fragment usually occurs at $pK_a = 2.5$,[10] however, we have not observed it under our experimental conditions. Double protonation of bipyridine results in repulsive interaction between the two positive charges and leads to a torsion angle of at least 40°, which is unlikely to occur within the cavity of **1**.

In contrast, the absorption spectrum of **2@1** exhibits only one isosbestic point at $\lambda =$ 332 nm (Figure S1 in the Supporting Information) that relates to the bipyridine part, with a remarkably high pK_a value of 8.1. The absence of a second isosbestic point is not surprising because deprotonation of both the bipyridinium and the ammonium group is expected to result in dissociation of the complex. It has already been reported that the pK_a values of bis-ammonium guest

Table 1. Spectral properties of bipyridine ligands **2** and **3** and their complexes with **1** (298 K, pH 3).

	Absorption		Emission
	λ_{max} [nm]	ε_{max} [$M^{-1}cm^{-1}$]	λ_{max} [nm]
2	287	12000	417
	353	17000	
2@1	302	4000	455
	371	9000	
3	254	8900	453
	302	11000	513
	377	15000	
3@1	305	6400	455
	371	8000	

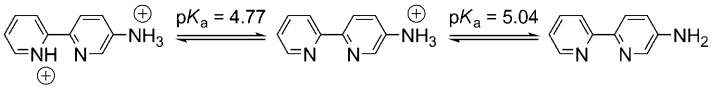

Scheme 2.

molecules increase upon formation of host–guest complexes with CB[*n*], as expected for a binding mode that is largely composed of charge–dipole interactions.[5c]

The emission spectrum of **2** ($\lambda_{ex} = 360$ nm) is characterized by an intense band at $\lambda = 417$ nm with tailing up to $\lambda =$

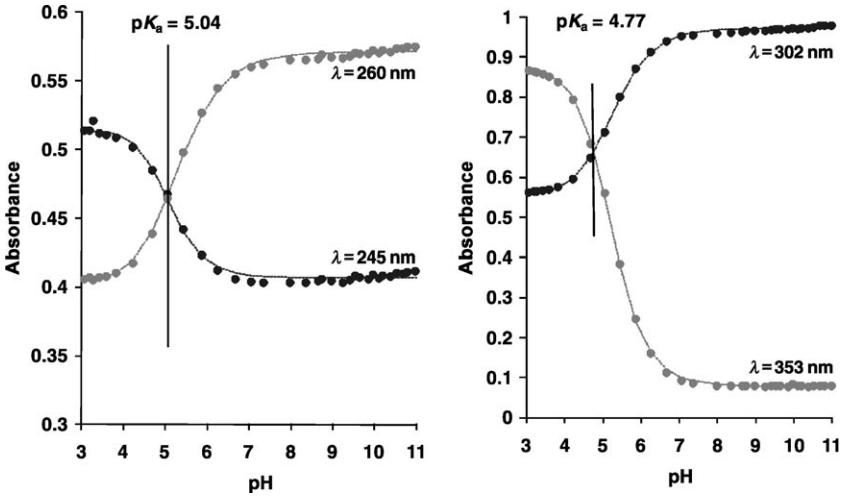

Figure 2. Determination of the pK_a values of **2** by monitoring the changes in its UV/Vis absorbance at $\lambda = 245$ and 260 nm (left) and at $\lambda = 302$ and 353 nm (right). The absorbance intensity changes were recorded for pH values of 3–11.

455 nm, which can be ascribed to locally excited and charge transfer excited states, respectively (Figure S2 in the Supporting Information).[11] The emission of doubly protonated **2** at pH 3 is 300 times more intense than that of the neutral molecule at pH 10. This phenomenon is expected because the nonbonding electrons of the amine group in the neutral molecule can efficiently quench the excited state. Accordingly, monitoring the emission intensity at $\lambda = 417$ nm as a function of pH between 3 and 9 allowed us to determine the pK_a of the amine group as 5.65 ± 0.05. The second pK_a (≈ 4.35) could also be determined by a similar analysis of another very small variation in the fluorescence intensity as a function of pH (Figure S2, upper inset, in the Supporting Information).

In contrast, the emission spectrum of **2@1** ($\lambda_{ex} = 360$ nm) is characterized by an intense band at $\lambda = 455$ nm with essentially no tailing, which probably arises from a dominant intramolecular charge transfer excited state (Figure 3). The emission of doubly protonated **2@1** at pH 3 is about 200 times more intense than that of free **2** at pH 10. Monitoring the emission intensity at $\lambda = 455$ nm as a function of pH allowed for determination of the pK_a of the bipyridine group (7.45 ± 0.05). It has been suggested that when molecules in solution are continuously excited, their acid–base equilibrium is strongly dependant on the reversible formation of an internal charge transfer excited state (S_1^{ICT}).[11] Thus, the observed increased acidity of the bipyridine unit in the excited state of **2@1** (p$K_a = 7.45$) in comparison with that of the ground state (p$K_a = 8.1$) can be explained by an internal charge transfer. A similar behavior was observed with **2**, in which the bipyridine unit was more acidic in the excited state (p$K_a = 4.35$) than in the ground state (p$K_a = 4.77$).

The remarkable pK_a shift between the free and bound ligand, **2** versus **2@1**, in either the ground state ($\Delta pK_a = 3.3$, Figure 4) or the excited state ($\Delta pK_a = 3.1$) highlights the strong charge–dipole interaction upon binding (Table 2). Consequently, **2@1** can be conveniently used as a fluorescent sensor within a broad range of over 3 pK_a units in which the complex is doubly protonated and highly fluorescent whereas the free ligand is neutral and essentially nonfluorescent.

Compound **3** and its complex **3@1** exhibit essentially the same UV/Vis absorption spectrum with no redshift of the latter (Figure S3 in the Supporting Information and Figure 5). The pH dependence of these spectra is much more complex than those of **2** and **2@1** because **3** contains four protonation sites and is conformational-

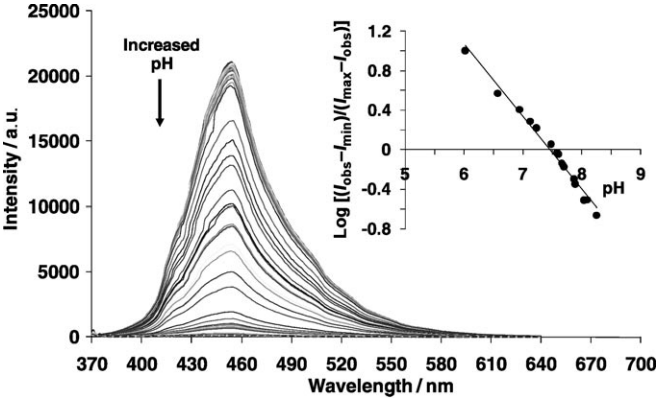

Figure 3. Effect of pH on the fluorescence intensity of **2@1** ($\lambda_{ex} = 360$ nm). Inset: Evaluation of the pK_a value by using a logarithmic linear regression plot: $pK_a = pH - \log[(I_{obs} - I_{min})/(I_{max} - I_{obs})]$; $y = -0.7387x + 5.5064$, $R^2 = 0.9849$.

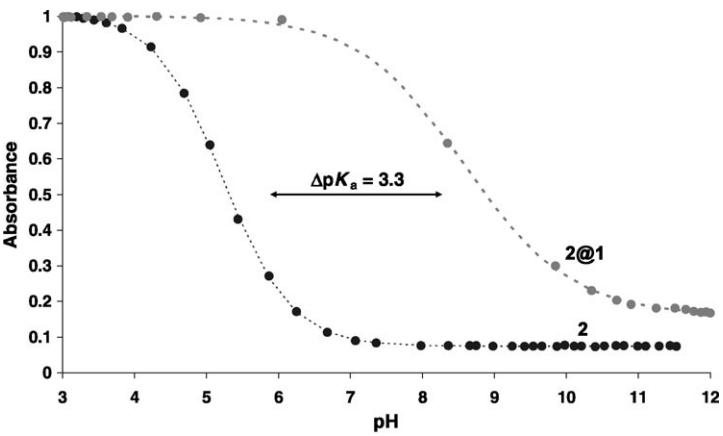

Figure 4. A comparison of the UV/Vis absorption of **2** ($\lambda_{max} = 362$ nm, normalized) and **2@1** as a function of pH. The dashed lines represent curve fittings by using a simple iterative least-squares analysis: $I_{obs} = [I_{max}(10^{(pH-pKa)}) + I_{min}]/(1+10^{(pH-pKa)})$.

Table 2. pK_a values of free **2** and **3** and bound **2@1** and **3@1** at 298 K.

	Ground state pK_a	Excited state pK_a
2	4.77	≈4.35
	5.04	5.65
2@1	8.10	7.45
3	4.38	5.20
	4.8, 5.24	6.05
3@1	7.53	6.80[a]

[a] Average value (see text).

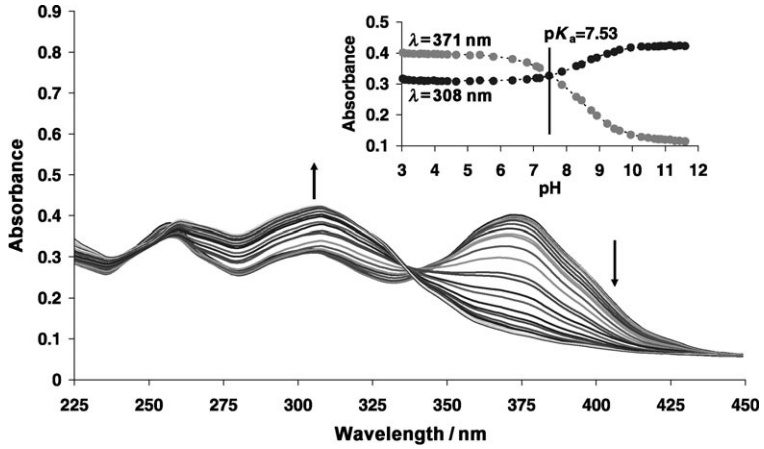

Figure 5. UV/Vis absorption spectra of **3@1** as a function of pH at 298 K exhibiting an isosbestic point at $\lambda=$ 341 nm. Arrows indicate intensity changes as the pH was increased from 3 to 12. Inset: Absorbance changes at $\lambda=308$ and 371 nm reveal a pK_a value of 7.53.

ly more flexible. The spectrum of **3@1** exhibits the same pH-dependence trend seen with **2** and **2@1** (increased intensity of the high energy π–π* absorption and decreased intensity of a low-energy band along with one isosbestic point), whereas the spectrum of **3** exhibits three bands ($\lambda_{max}=254$, 302, and 377 nm), all of which decrease in intensity as the pH increases. The pH dependence of the $\lambda=377$, 254, and 302 nm absorption maxima allowed for determination of three pK_a values of 4.38, 4.80, and 5.24, respectively (Table 2 and Figure S3 in the Supporting Information). We assume that the pK_a value of 4.38 is associated with simultaneous protonation of both bipyridine units, whereas the two other values reflect sequential protonation of the two amine groups.

As was the case for **2@1**, the spectral dependence of **3@1** on the pH allowed us to determine only the pK_a of the bipyridine moiety. Thus, monitoring the intensity of the bands at $\lambda=308$ and 371 nm, which are separated by an isosbestic point at $\lambda=341$ nm, gave a pK_a value of 7.53 (Figure 5). Again, as was the case for **2@1**, the notable pK_a shift ($\Delta pK_a=3.15$) highlights the strong charge–dipole interaction as the main binding mechanism between **3** and **1**.

The emission spectrum of **3**, which is far more complex than the emission spectrum of **2**, exhibits dual fluorescence bands at $\lambda=455$ and 510 nm (Figure 6). Although the $\lambda=$ 455 nm emission is reminiscent of the broad $\lambda=417$ nm band of **2**, including the ICT tailing, the additional broad emission at $\lambda=510$ nm is quite unusual.[12] It can be explained by excimer formation, which is known for many aromatic hydrocarbons, such as 1,4-bis(4′-pyridylethynyl)benzene[13] and 2,2′-bipyridine in silica gel glass,[14] which exhibit excimer fluorescence in solution at room temperature. Intramolecular excimer fluorescence is known in molecules that have two or more identical aromatic groups (segmers) linked by a flexible tether.[15] If an excited-state segmer can move into the vicinity of a ground-state segmer during the lifetime of the excited state, it may form an intramolecular excimer ($^1D^*$) that is characterized by structureless fluorescence spectrum at lower energy than the monomeric emission. The observed excimer fluorescence of **3** seems to reflect an effective π–π stacking between two segmers, one of which is in the excited state. The intensity of this high-energy band is slightly dependent on pH within the range of 6–10, and reveals a pK_a value of 5.20± 0.05 ($\lambda_{ex}=360$ nm, $\lambda_{em}=$ 455 nm; Table 2) associated with protonation of the bipyridine unit. The lower transition

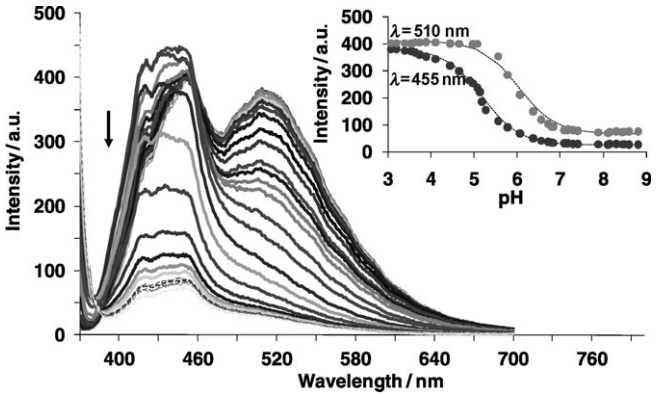

Figure 6. Effect of pH on the fluorescence intensity of **3** ($\lambda_{ex}=360$ nm). Inset: The effect on the monomer emission at $\lambda=455$ nm and the excimer emission at $\lambda=510$ nm.

energy band followed a similar decrease but at higher pH. Thus, the variation in emission at $\lambda=510$ nm with pH revealed a pK_a value of 6.05±0.05, which is probably associated with protonation of the amine groups.

Excimer emission is totally prevented upon formation of either the 1:2 or the 1:1 complex of **3@1** because the two segmers are now shielded from one another by the host molecule and by the loss of conformational flexibility. Thus, the emission spectrum of **3@1** exhibits only the monomeric emission band at $\lambda=450$ nm (Figure 7), which is similar to

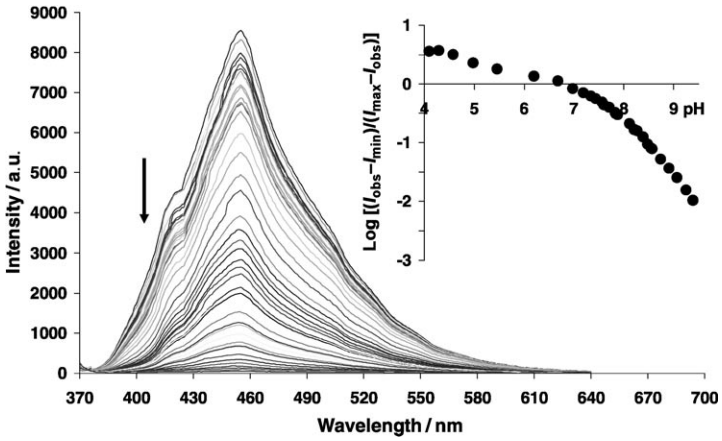

Figure 7. Effect of pH on the fluorescence intensity of **3@1** ($\lambda_{ex}=360$ nm, $\lambda_{em}=455$ nm). Inset: Determination of the pK_a value (Table 2) was carried out by using the acid–base isotherm equation given in Figure 3.

the spectrum of **2@1**. As in the case of **2@1**, the pH dependence of the emission intensity of **3@1** revealed a pK_a value of 6.80 ± 0.05 (Table 2) associated with protonation of the bipyridine unit, which is lower than the pK_a value of the ground state (7.53 ± 0.05). This effect can be explained by excited state acidity enhancement of the bipyridine units when hosted within **1**. It should be noted, however, that the logarithmic isotherm is not perfectly linear; this reflects multiple protonations. Because it was not possible to differentiate between the various acid–base equilibria, the observed pK_a should be considered as an average value.

Addition of **1** to a buffered aqueous solution (NH_4OAc, pH 7.0) of either **2** or **3** resulted in remarkable fluorescence enhancement factors of 30 and 24, respectively (Figure 8 and Figure S4 in the Supporting Information). We used the continuous variation plot[16] to verify the 1:1 binding stoichiometry between **2** and **1** (Figure S5 in the Supporting Information). By using the Hill plot[17] for the titration curve of **2** by **1**, the host–guest binding constant was obtained ($\log\beta=5.70\pm0.02$).[18] This value of binding constant remained unchanged over a broad pH range of between 2 and 7. Unlike the case of **2**, the titration of **3** by **1** indicated a binding stoichiometry of 1:2, as revealed by the Job plot[19] (Figure S6 in the Supporting Information). To obtain the **3@1** binding constant we used a model of two identical noninteracting binding sites[20] to give the overall binding constant of $\log\beta=5.07\pm0.02$. Apparently, monoalkylation of the amine group on going from **2** to **3** introduces steric demands that diminish the binding efficiency. Moreover, considering the fact that 1,4-bis(aminomethyl)benzene is a strong binder of CB,[6,21] our observation that the central portion of **3** is a weaker binder than its peripheral bipyridine moieties indicates that alkylation of 1,4-bis(aminomethyl)benzene significantly reduces its binding affinity to **1**.

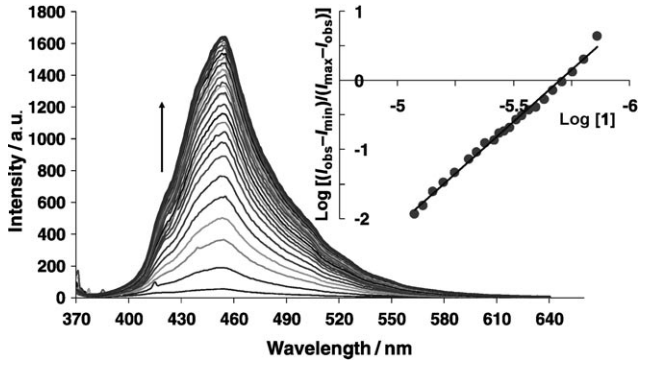

Figure 8. Changes in the emission spectrum of **2** ($\lambda_{ex}=360$ nm, $\lambda_{em}=455$ nm) upon addition of **1**. A buffered solution of **1** (NH_4OAc, 0.1 mM, pH 7) was added in portions (20 μL each, 0.1 mM) to a solution of **2** (10 mL, 0.001 mM) at 298 K. Inset: Hill plot analysis that afforded the value of $\log\beta$ (5.70 ± 0.02); $y=-3.0028x-17.133$, $R^2=0.9938$.

We used isothermal titration calorimetry (ITC) measurements to independently determine the binding affinity and maximal binding stoichiometry between **1** and either **2** or **3** (Table 3 and Figures S7 and S8 in the Supporting Information). As can be seen from Table 3, the ITC data verified both binding constants and binding stoichiometry values (1:1 for **2@1** and 1:2 for **3@1**) that were obtained from the fluorescence enhancement experiments. To better understand the binding mode between **1** and **2**, we prepared two deaza analogues, **4** and **5**. Their binding constants to **1** were determined by using ITC and the data were compared with the known binding constant of 1,6-diaminohexane (**8**).[21] The binding constant of **4** is quite similar to that of **2**, which indicates a double interaction with both portals of **1**. In contrast, compound **5** binds weakly to **1** and is apparently incapable of interacting with both portals simultaneously (Table 3 and Figure S9 in the Supporting Information). This interaction did not produce any notable spectral signature; no change was observed in the absorption spectrum ($\lambda_{ex}=255$ nm), and only a 20% increase was noticed in the emission spectrum ($\lambda_{em}=325$ nm).

Table 3. Overall binding constants ($\log\beta$), binding stoichiometry (n), enthalpy (ΔH), and entropy (ΔS) of binding for host–guest complexes **2@1**, **3@1**, **4@1**, **5@1**, and **8@1**.[a]

Host–Guest	Conditions	$\log\beta$[18]	n	ΔH [Kcal mol^{-1}]	ΔS [eu]
2@1	A	5.49 ± 0.02	0.87	-13.79 ± 0.01	-20.4 ± 0.2
	B	4.87 ± 0.01	0.96	-12.18 ± 0.01	-18.7 ± 0.1
3@1	A	5.34 ± 0.04	0.44	-20.64 ± 0.03	-43.6 ± 0.2
4@1	A	4.80 ± 0.02	0.96	-8.0 ± 0.1	-4.4 ± 0.2
5@1	A	4.20 ± 0.05	0.45	-15.79 ± 0.18	-32.9 ± 0.2
8@1	A	6.25 ± 0.04	0.91	-11.13 ± 0.01	-8.1 ± 0.02
	B	6.59 ± 0.05	0.86	-10.35 ± 0.01	-4.6 ± 0.03

[a] [**1**] = 0.13 mM for all experiments. Conditions: A) [Ligand] = 1 mM in NH_4Cl buffer (10 mM, pH 4, 303 K). B) [**2**] = 1.6 mM and [**8**] = 1 mM in NH_4OAc buffer (10 mM, pH 7, 298 K).

In contrast, the ^{1}H NMR spectra exhibited a significant shift in the phenyl protons (≈1 ppm upfield) upon binding to **1**, whereas the signals that correspond to the protons *ortho* to the amine group were not affected. These observations reflect an interesting binding mode of **5** in which the

phenyl group is incorporated within the cavity of **1**, with preferred interaction between the CB portal and the pyridine function rather than with the amine group. The 1:2 binding stoichiometry between **5** and **1** confirms that one molecule of **1** interacts with the pyridine ring and another molecule interacts with the amine group. This unique behavior is consistent with the reported basicity of 3-aminopyridine in aqueous solution, in which the first protonation site is the pyridine nitrogen atom.[22]

Formation of host–guest complexes **2@1** and **3@1** was found to involve not only significant increase in fluorescence intensity but also a remarkable enhancement of the quantum yields. The quantum yield of free **2** and **3** in the absence of **1** was found to be 0.89 and 0.45, respectively, whereas the quantum yields of their inclusion complexes with **1** became quantitative (1.00; Table 4 and Figure S10 in the Supporting Information). This effect could probably arise from the restricted motion of the guest molecules within the tight cavity of **1**. It has been previously proposed that the relatively high quantum yields (0.95 and 0.94) observed for 4,4′-bis[(2,5-dimethoxyphenyl)ethynyl]biphenyl and 4,4′-bis[(2,5-dimethoxyphenyl)ethynyl]-2,2′-bipyridine, respectively, reflected their rigid structures.[23] The enhanced quantum yield could also result from a strong polar medium effect and desolvation of the guest molecule on moving from an aqueous medium to the hydrophobic environment of the host. In contrast, very small variations in the fluorescence lifetime of the free and bound guests were observed that were within the most usual range of between 1 and 10 ns. The diversity of the lifetime parameter exhibited only minor fluctuations, particularly in comparison with other parameters, such as energy bands, intensities, and quantum yields.

Table 4. Fluorescence quantum yields (Φ_F) and fluorescence lifetime (τ) values (aqueous HCl, pH 3) for **2**, **2@1**, **3**, and **3@1**. The Φ_F values were determined by applying the comparative method[32] with coumarin-1 as the standard and correcting for the solvent refractive index ratio (0.959; see the Supporting Information).

	τ [ns]	Φ_F
2	7.8	0.89
2@1	7.6	1.00
3	7.6	0.45
3@1	10.1	1.00
Coumarin[33]	4.3 (EtOH)	0.70 (EtOH)

To demonstrate the concept of interconnected equilibria networks, we constructed a system that was comprised of five components (**A**–**E**) that were added sequentially to a buffered aqueous solution (10 mM NH_4OAc, pH 7.0, 298 K). The resulting noncovalent binding events were monitored by measuring the fluorescence intensity (Scheme 3 and Figure 9). This "chemical food chain" started with the addition of component **B** (represented by **2**) to a solution that contained component **A** (represented by **1**) and formation of the highly fluorescent inclusion complex **2@1**. Addition of the third component (**C**; represented by $Cu(OAc)_2$) resulted in complete suppression of the fluorescence intensity,

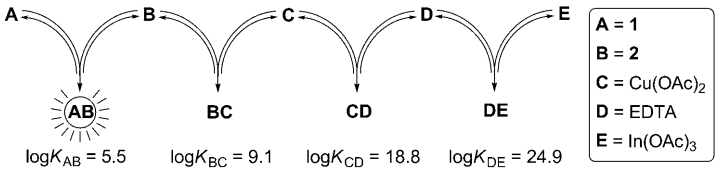

Scheme 3. A series of interconnected equilibria, a chemical food chain composed of five components.

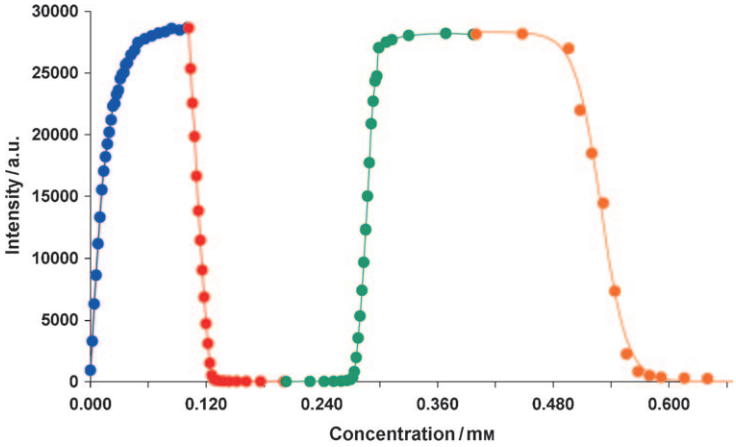

Figure 9. A chemical food chain monitored by using fluorescence intensity ($\lambda_{ex}=360$ nm, $\lambda_{em}=455$ nm). The concentration scale refers to the sequential additions of all four components to a solution of **1** (0.1 mM; 10 mM NH_4OAc, pH 7). The blue curve indicates stepwise addition of **2** (up to 0.1 mM). The red curve indicates stepwise addition of Cu^{+2} acetate (up to 0.2 mM). The green curve indicates stepwise addition of EDTA (up to 0.2 mM). The orange curve indicates stepwise addition of In^{+3} acetate (up to 0.2 mM).

which indicates quantitative dissociation of **2** from **1** with concomitant formation of the expected 1:2 complex of Cu^{II} with **2** (for evidence for the 1:2 stoichiometry, see the Supporting Information and Figure S11). This complex formation was associated with complete quenching even of the independent, relatively low fluorescence of **2**, as was evident from a control experiment in which addition of $Cu(OAc)_2$ to an aqueous solution of **2** in the absence of **1** resulted in a decrease in the fluorescence intensity by two orders of magnitude. Addition of the fourth component (**D**) represented by ethylenediaminetetraacetic acid (EDTA), which is a strong binder of Cu^{II} ($\log\beta=15.5$),[24] resulted in complete release of **2**. Compound **2** was thus once again made available for interaction with **1** and the maximal fluorescence intensity of **2@1** was recovered. Finally, addition of the fifth component (**E**) represented by $In(OAc)_3$ resulted in quantitative formation of the expected In^{III}@EDTA complex ($\log\beta\approx25$).[25] The released Cu^{II} ions then became available to regenerate the **BC** complex with concomitant dissociation of the **AB** (**2@1**) complex and complete suppression of the fluorescence intensity (Scheme 3 and Figure 9).

The complexation-dependent fluorescence phenomenon provides an opportunity to quantitatively determine the binding constants between **1** and other ligands through com-

petitive binding experiments. This approach allows for monitoring "dark" binding events that by themselves are not associated with any significant change in either UV/Vis absorption or fluorescence intensity. Typical examples are the formation of the inclusion complexes between **1** and saturated diamine compounds, such as putrecine (**6**), cadaverine (**7**), and 1,6-diaminohexane (**8**).[26,27] To demonstrate this advantage we carried out displacement titration experiments with **6**–**8** (Figures S12 and S13 in the Supporting Information and Figure 10, respectively). Plotting the competitive binding data by using the appropriate model (see details in the Supporting Information) with the above-mentioned binding constant of **2@1** ($\log\beta = 5.70$) gave the binding constants of **6@1** ($\log\beta = 6.9$), **7@1** ($\log\beta = 8.1$), and **8@1** ($\log\beta = 7.49$). These values are comparable with the values that were measured by other methods, such as ^{1}H NMR spectroscopy, for **6@1** ($\log\beta = 7.3$),[26] **7@1** ($\log\beta = 7.6$–8.2), and **8@1** ($\log\beta = 6.44$–8.46).[21a,26,27] The only precedent for monitoring a dark binding event between a UV-inactive guest and CB[6] has been reported by Nau[5c] for a carbazole fluorophore covalently linked to diaminoalkane. Because the fluorophore in the tethered conjugate only indirectly interacts with the host, the fluorescence intensities might be more susceptible to background noise and to undesired quenching by interfering analytes.

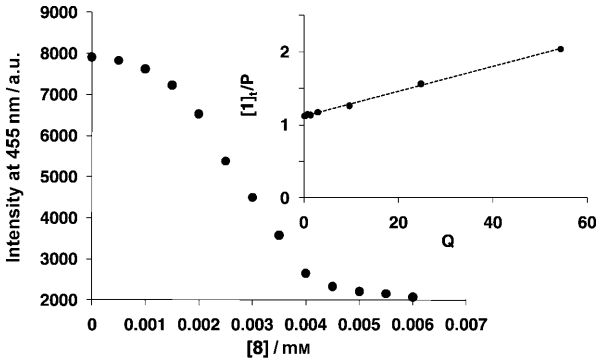

Figure 10. Determination of binding constant of **8@1** by competition binding. The fluorescence intensity of **2** ($\lambda_{ex} = 360$ nm, $\lambda_{em} = 455$ nm) was measured as a function of the stepwise addition of **8** (in 10 mM NH_4Cl, pH 3 buffer) to an aqueous solution of **2@1** (0.03 mM, in 0.1 mM NH_4Cl, pH 3 buffer). Inset: Determination of the binding constant for **8@1** was obtained from the equation: $[\mathbf{1}]_t/P = 0.017Q + 1.1$, $R^2 = 0.9983$, $\mathrm{Log}\,K_{\mathbf{8@1}} = 7.47$ (for details, see the Supporting Information).

Another attractive application of the complexation-dependent fluorescence of **2@1** is the ability to rapidly monitor biocatalytic reactions, including quantitative determination of their kinetic parameters.[28] We demonstrated this advantage by quantitatively monitoring the hydrolysis of amide **20** as catalyzed by penicillin G acylase (PGA) and the β-elimination reaction of β-cabamoyloxy ketone **21** as catalyzed by aldolase antibody 38C2 (Scheme 4).

Substrate **20** was prepared in high yield by dimethylaminopyridine-catalyzed acylation of **2** with phenylacetyl chloride in dichloromethane. Substrate **21** was prepared from ethyl propioacetate (**22**; Scheme 5). Protection of the ketone group followed by $LiAlH_4$ reduction afforded alcohol **23**, which was converted to active imidazolyl carbamate **24**. Transamidation of the latter by using compound **9** afforded stable carbamate **25**. Stille coupling with 2-(tributyltin)pyridine and palladium(0) catalyst afforded bipyridine derivative **26**. Finally, deprotection of the ketone group afforded **21**.

Both biocatalytic reactions were carried out in the presence of excess **1**, which did not interfere with the catalytic activity of either PGA or 38C2 as verified by control experiments. Substrates **20** and **21** were designed to release **2** as one of the biocatalytic reaction products. The rapid formation of highly fluorescent complex **2@1** upon release of **2** allowed for fast, quantitative monitoring of the progress of both reactions by using the appropriate calibration curves of fluorescence intensity versus [**2**]. Because the initial rates within the first 2 min of the reaction were monitored by using fluorescence intensity ($\lambda_{ex} = 360$ nm, $\lambda_{em.} = 453$ nm), it was possible to carry out all reactions in a very small

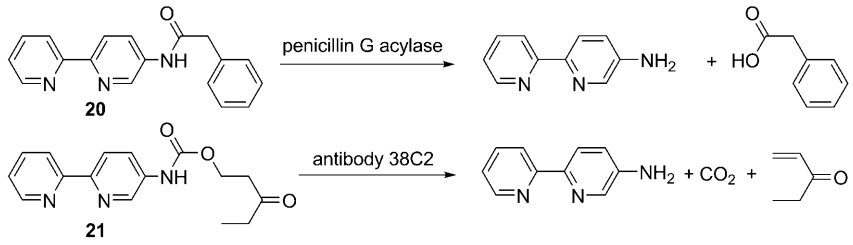

Scheme 4.

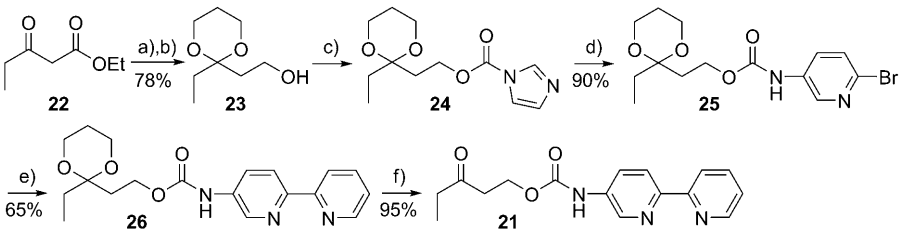

Scheme 5. Synthesis of substrate **21**. Reagents and conditions: a) 1,3-propanediol, *p*-TsOH (cat.), benzene, reflux, 20 h; b) $LiAlH_4$, Et_2O, reflux, 5 h; c) carbonyldiimidazole, CH_2Cl_2, RT, 2 h; d) 5-amino-2-bromopyridine, NaH, THF, RT, 16 h; e) 2-(tributyltin)pyridine, $[Pd(PPh_3)_4]$, toluene, 120 °C, 24 h; f) AcOH, H_2O, RT, 16 h.

volume (250 μL) by using a 96-well plate and a fluorescence microplate reader.

The PGA-catalyzed reactions were carried out in phosphate-buffered saline (PBS, pH 7.4) at 25 °C by using a fixed concentration of the enzyme (7.14 nM) and eight different concentrations of **20** (0.025–0.075 μM) in the presence of **1** (0.08–0.24 μM). The kinetic parameters ($k_{cat.}=6.54\times10^4\ min^{-1}$, $k_{cat.}/k_{uncat.}=2.9\times10^8$, $K_m=0.884$ μM, $k_{cat.}/K_m=7.4\times10^4\ min^{-1}$) were obtained by a Lineweaver–Burk analysis of the measured initial rates (Figure 11). These kinetic parameters indicate that the PGA-catalyzed hydrolysis of **20** is 40 times faster than that of 6-nitro-3-phenylacetamidobenzoic acid (NIPAB; $k_{cat.}=1.62\times10^3\ min^{-1}$, $K_m=11$ μM, $k_{cat.}/K_m=1.47\times10^2\ \mu M^{-1}s^{-1}$),[29] which is commonly used for determining the catalytic activity of PGA samples.

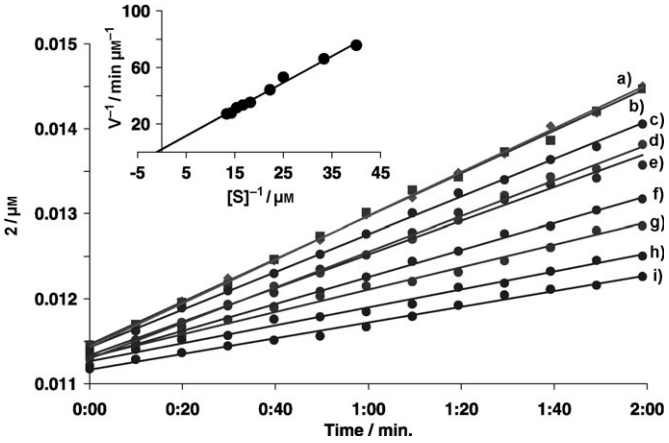

Figure 11. The kinetics of the PGA-catalyzed hydrolysis of **9** as monitored by using fluorescence intensity ($\lambda_{ex}=360$ nm, $\lambda_{em}=453$ nm). The concentrations of **2** (a) 0.075, b) 0.070, c) 0.065, d) 0.060, e) 0.055, f) 0.045, g) 0.040, h) 0.030, i) 0.025 μM) were determined by using a calibration curve (not shown). All reactions were carried out in PBS, pH 7.4, 25 °C by using PGA (7.14 nM) varying concentrations of substrate. Inset: Determination of $k_{cat.}$ ($6.54\times10^4\ min^{-1}$) and K_m (884 μM) by using a Lineweaver–Burk analysis; $y=1.893x+2.1406$, $R^2=0.9908$, $V_{max}=0.467\ \mu M\,min^{-1}$.

The 38C2-catalyzed reactions were carried out in a similar fashion by using a fixed concentration of aldolase antibody 38C2 (1.5 μM) and eight different concentrations of **21** (0.025–0.075 μM) and **1** (0.08–0.24 μM) to give the kinetic parameters ($k_{cat.}=9.9\ min^{-1}$, $k_{cat.}/k_{uncat.}=1.5\times10^3$, $K_m=0.04$ mM; Figure S14). It is interesting to compare these parameters with those of similar substrates studied earlier with the same antibody. Although the value of $k_{cat.}$ of **21** is slightly higher than the value of the best substrate studied so far, 3-(*N*-phenylcarbamoyl)cyclohexanone ($k_{cat.}=8.9\ min^{-1}$, $K_m=1.27$ mM),[30] the much smaller K_m value observed with **21** suggests that aminobipyridine derivatives are tight binders of aldolase antibody 38C2. Hence, the presence of **1** in the reaction mixture has a beneficial effect on the catalytic reaction in that it scavenges **2** and thereby prevents product inhibition of the catalyst.

Conclusion

4-Aminobipyridine derivatives form strong inclusion complexes with **1** and exhibit remarkably large enhancements of fluorescence intensity and quantum yields. The remarkable complexation-induced pK_a shift ($\Delta pK_a=3.3$) highlights the strong charge–dipole interaction upon binding. This enhanced fluorescence phenomenon can be used for the design of switchable beacons that can be incorporated into cascades of binding networks. This concept has been demonstrated herein by three different applications: 1) a switchable fluorescent beacon for chemical sensing of transition metals and ligands; 2) direct measurement of binding constants between **1** and other, non-fluorescent guest molecules; and 3) quantitative monitoring of biocatalytic reactions and rapid determination of their kinetic parameters. Further applications of these phenomena in multiparameter systems are currently underway in our laboratories, including the construction of chemical logic gates, fast screening of libraries of ligands of transition metals, fast measurement of metal–ligand binding constants, and further expansion of the interconnected binding networks.

Experimental Section

General methods: All reactions were carried out in anhydrous solvents under an inert atmosphere. Compounds **9**, **10**, and **22** were purchased from Aldrich Chemicals. CB[6] **1** was prepared as described before.[3a] PGA and catalytic antibody 38C2 were purchased from Aldrich in the form of lyophilized powder. Flash chromatography was performed on Merck silica gel 60 (230–400 mesh). ^1H and ^{13}C NMR spectra were recorded in the solvents indicated by using an AVANCE 500 Bruker spectrometer. Chemical shifts (δ) are given in ppm relative to TMS. The residual solvent signals were used as references and the chemical shifts were converted to the TMS scale: $CDCl_3$: $\delta_H=7.26$ ppm, $\delta_C=77.16$ ppm; D_2O/DCl (with trace DMSO): $\delta_H=2.71$ ppm, $\delta_C=39.4$ ppm. Mass spectra were recorded by using either Waters MALDI microMX (TOF) or Waters LCT Premier microMax spectrometers (TOF-ESI, with MeCN/H_2O 1:1). ITC measurements were performed at either 298 or 303 K by using a VP-ITC instrument (MicroCal, USA). UV absorption and fluorescence spectra for binding studies were recorded at 25 °C by using a SpectraMax M2 spectrometer. Quantum yield measurements were determined by using a Fluorolog 3-21 fluorimeter equipped with a Hamamatzu R928 photomultiplier. Emission spectra were acquired following excitation at the given wavelength and were corrected for the wavelength dependence of the photomultiplier tube. Lifetime measurements were carried out by using a continuum Nd–Yag Laser 7010 Model at the third harmonic, $\lambda=355$ nm, as the exciting source and applying a pulse width of 5 ns. The laser was equipped with a Spectra-Pro 275 monochromator, a Hamamatzu R928 photomultiplier, and a Tekronix TDS 220 scope controller. Data were processed by using LabVIEW software (National Instruments, USA).

1-(2-Bromopyridine-5-yl)-2,5-dimethyl-1*H*-pyrrole (11): *p*-TsOH (15 mg, 0.08 mmol) was added to a stirred solution of **9** (1 g, 5.8 mmol) and 2,5-hexanedione (0.75 mL, 6.4 mmol) in toluene (20 mL), and the mixture was heated at reflux for 4 h by using a Dean–Stark apparatus. After cooling, the mixture was quenched with saturated aq $NaHCO_3$ and extracted with toluene (2×20 mL). The organic phase was washed with H_2O and brine, dried over $MgSO_4$, and the solvent was removed under reduced pressure. The resulting crude product was purified by column chromatography (silica gel, hexane/EtOAc 9:1) to give pure **11** as a yellowish solid (1.4 g, 97 %). ^1H NMR (500 MHz, $CDCl_3$): $\delta=8.29$ (d, $J=2.5$ Hz, 1H),

7.61 (d, $J=8$ Hz, 1H), 7.44 (dd, $J=8$, 2.5 Hz, 1H), 5.95 (s, 2H), 2.05 ppm (s, 6H); ^{13}C NMR (125 MHz, $CDCl_3$): $\delta=149.4$, 140.7, 138.0, 135.0, 128.8, 128.4, 107.0, 12.0 ppm; MS (TOF-ES): m/z calcd for $C_{11}H_{11}BrN_2$: 250; found: 249 $[M-H]^+$.

1-(4-Iodophenyl)-2,5-dimethyl-1*H*-pyrrole (12): Synthesis was carried out by using **10** (1.3 g, 6 mmol), 2,5-hexanedione (0.8 mL, 6.6 mmol), *p*-TsOH (20 mg) in toluene and by following the same procedure as described for **11**. Column chromatography of the crude product (silica gel, hexane/EtOAc 9:1) afforded **12** as a yellowish solid (1.73 g, 97%). ^{1}H NMR (500 MHz, $CDCl_3$): $\delta=7.79$ (d, $J=8$ Hz, 2H), 6.96 (d, $J=8.5$ Hz, 2H), 5.9 (s, 2H), 2.02 ppm (s, 6H); MS (TOF-ES): m/z calcd for $C_{12}H_{12}IN$: 297; found: 296 $[M-H]^+$.

1-(2,2′-Bipyridine-5-yl)-2,5-dimethyl-1*H*-pyrrole (13): 2-(Tributyltin)pyridine[31] (1.6 g, 4.5 mmol) in toluene (15 mL) was added to a stirred solution of **11** (0.75 g, 3 mmol), followed by addition of $[Pd(PPh_3)_4]$ (70 mg, 0.06 mmol) under argon at RT. After purging with argon for 15 min, the mixture was heated at 130°C for 24 h, then quenched with 2N NaOH and extracted with EtOAc. The organic phase was washed with brine, dried over Na_2SO_4, and the solvent was removed under reduced pressure. Column chromatography of the residue (silica gel, hexane/EtOAc 8:2) afforded **13** as a white solid (0.61 g, 82%). ^{1}H NMR (500 MHz, $CDCl_3$): $\delta=8.71$ (d, $J=4$ Hz, 1H), 8.57 (d, $J=2$ Hz, 1H), 8.54 (d, $J=8.5$ Hz, 1H), 8.44 (d, $J=8$ Hz, 1H), 7.86 (ddd, $J=7.5$, 8, 1.5 Hz, 1H), 8.68 (dd, $J=8.5$, 2.5 Hz, 1H), 7.35 (dd, $J=7$, 5 Hz, 1H), 5.96 (s 2H), 2.09 ppm (s, 6H); ^{13}C NMR (125 MHz, $CDCl_3$): $\delta=155.2$, 155.1, 149.3, 148.3, 137.1, 136.3, 135.5, 129.0, 124.0, 121.2, 121.2, 106.7, 13 ppm; MS (TOF-ES): m/z calcd for $C_{16}H_{15}N_3$: 249; found: 250 $[M+H]^+$.

2-[4-(2,5-Dimethyl-1*H*-pyrrol-1-yl)phenyl]pyridine (14): The synthesis was carried out by using compound **12** (700 mg, 2.35 mmol), 2-(tributyltin)pyridine (1.3 g, 3.5 mmol), and $[Pd(PPh_3)_4]$ (55 mg, 0.047 mmol) in toluene (15 mL), and by following the same procedure as described for **13**. The crude product was purified by column chromatography (silica gel, hexane/EtOAc 8:2) to give **14** as a white solid (466 mg, 80%). ^{1}H NMR (500 MHz, $CDCl_3$): $\delta=8.63$ (d, $J=2$ Hz, 1H), 8.00 (d, $J=6.5$ Hz, 2H), 7.70–7.68 (m, 2H), 7.24 ($J=6.5$ Hz, 2H), 7.19–7.16 (m, 1H), 5.84 (s, 2H), 1.20 ppm (s, 6H); ^{13}C NMR (125 MHz, $CDCl_3$): $\delta=156.5$, 149.7, 139.5, 138.6, 136.9, 128.7, 128.4, 127.6, 122.3, 120.5, 105.9, 13.0 ppm; MS (TOF-ES): m/z calcd for $C_{17}H_{16}N_2$: 248; found: 249 $[M+H]^+$.

5-Amino-2,2′-bipyridine hydrochloride (2): A mixture of **13** (500 mg, 2 mmol), hydroxylamine hydrochloride (1.5 g, 20 mmol), Et_3N (0.6 mL), EtOH (6 mL), and H_2O (2.6 mL) was heated at reflux for 24 h. After being cooled to RT, the mixture was quenched with cold 1N HCl (10 mL) and washed with iPr_2O, then the pH was adjusted to 9–10 by careful addition of 6N NaOH. The aqueous phase was extracted five times with CH_2Cl_2 and the combined organic phases were dried over Na_2SO_4. After removal of the solvent, the brown residue was dissolved in MeOH and a few drops of concd HCl were added to give the product as a white precipitate. The addition of Et_2O resulted in additional precipitation of **2** as a light-yellow solid (291 mg, 85%). ^{1}H NMR (500 MHz, D_2O/DCl): $\delta=8.67$ (d, $J=5.5$ Hz, 1H), 8.39 (dt, $J=1.5$, 6.5 Hz, 1H), 8.25 (d, $J=8$ Hz, 1H), 8.23 (d, $J=2.5$ Hz, 1H), 8.08 (d, $J=9$ Hz, 1H), 7.80 (t, $J=6$ Hz, 1H), 7.55 ppm (dd, $J=2.5$, 6.5 Hz, 1H); ^{13}C NMR (125 MHz, D_2O/DCl): $\delta=148.3$, 145.9, 145.2, 144.3, 137.1, 135.4, 126.9, 126.1, 125.2, 123.4 ppm; MS (TOF-LD): m/z calcd for $C_{10}H_9N_3$: 171; found: 172 $[M+H]^+$.

Inclusion complex of 1 with 2 (2@1): A solution of **1** (0.1 mmol) in H_2O (25 mL) was added to a solution of **2** (0.12 mmol) in acidic H_2O (25 mL, pH 3) and stirred at RT for 16 h. The resultant precipitate was removed by filtration, and the solvent of the filtrate was removed under reduced pressure. The residue from the filtrate was dissolved in H_2O (20 mL), then acetone (10 mL) was added and the resultant precipitate was washed with MeOH and Et_2O to give complex **2@1** in quantitative yield. ^{1}H NMR (500 MHz, D_2O/DCl): $\delta=8.80$ (d, $J=8.5$ Hz, 1H), 8.59 (d, $J=5.5$ Hz, 1H), 8.43 (t, $J=8$ Hz, 1H), 7.76 (t, $J=6.5$ Hz, 1H), 7.3 (d, $J=3$ Hz, 2H), 6.13 (d, $J=8.5$ Hz, 1H), 5.68 (dd, $J=81.5$, 15.5 Hz, 12H), 5.46 (s, 12H), 4.21 ppm (dd, $J=27$, 15.5 Hz, 12H); MS (TOF-ES): m/z calcd for $C_{46}H_{47}Cl_2N_{27}O_{12}$: 1239; found: 1169 $[M-2Cl-H]^+$.

4-(Pyridin-2-yl)benzenamonium chloride (4): The synthesis was performed by using **14** (310 mg, 1.25 mmol), hydroxylamine hydrochloride (900 mg, 12.5 mmol), Et_3N (0.35 mL), EtOH (6 mL), and H_2O (2.6 mL), and by following the above-described procedure for the preparation of **2**, and gave **4** as a light-brown solid (180 mg, 85%). ^{1}H NMR (500 MHz, D_2O/DCl): $\delta=8.75$ (d, $J=6$ Hz, 1H), 8.63 (dt, $J=1$, 7 Hz, 1H), 8.29 (d, $J=8$ Hz, 1H), 8.00 (t, $J=7$ Hz, 1H), 7.97 (d, $J=8.5$ Hz, 2H), 7.55 ppm (d, $J=8.5$ Hz, 2H); ^{13}C NMR (125 MHz, D_2O/DCl): $\delta=152.0$, 147.8, 141.8, 137.9, 130.6, 130.0, 126.8, 126.1, 123.4 ppm; MS (TOF-LD): m/z calcd for $C_{11}H_{10}N_2$: 170; found: 171 $[M+H]^+$.

Inclusion complex of 1 with 4 (4@1): Complex **4@1** was prepared by using the same procedure as described for **2@1**. ^{1}H NMR (500 MHz, D_2O/DCl): $\delta=8.89$ (d, $J=8.5$ Hz, 1H), 8.53 (d, $J=5.5$ Hz, 1H), 8.40 (t, $J=8$ Hz, 1H), 7.70 (t, $J=7$ Hz, 1H), 7.10 (d, $J=8.5$ Hz, 2H), 6.04 (d, $J=8.5$ Hz, 1H), 5.69 (dd, $J=68.5$, 15.5 Hz, 12H), 5.48 (s, 12H), 4.24 ppm (dd, $J=11.5$, 15.5 Hz, 12H); MS (TOF-ES): m/z calcd for $C_{47}H_{48}Cl_2N_{26}O_{12}$: 1240; found: 1168 $[M-2Cl-H]^+$.

2-Bromo-5-(bis-Boc)aminopyridine (15): A solution of **9** (1 g, 5.8 mmol) and Et_3N (2.5 mL, 17.4 mmol) in CH_2Cl_2 (50 mL) was stirred for 30 min at RT. $(Boc)_2O$ (2.8 g, 12.8 mmol) and DMAP (116 mg) in CH_2Cl_2 (5 mL) were added and the mixture was stirred overnight at RT, then quenched with aq NH_4Cl and extracted with CH_2Cl_2. The organic phase was separated and washed with H_2O and brine, dried over $MgSO_4$, and the solvent was removed under reduced pressure. The residue was purified by flash chromatography (silica gel, hexane/EtOAc 8:2) to give **15** as a colorless solid (1.84 g, 85%). ^{1}H NMR (300 MHz, $CDCl_3$): $\delta=8.19$ (d, $J=2.7$ Hz, 1H), 7.50 (d, $J=8.4$ Hz, 1H), 7.35 (dd, $J=5.7$, 2.7 Hz, 1H), 1.42 ppm (s, 18H).

2-Phenyl-5-(bis-Boc)aminopyridine (16): A mixture of **15** (750 mg, 2 mmol), phenylboronic acid (365 mg, 3 mmol), $CsCO_3$ (2 g, 6 mmol), and bis(tri-*tert*-butyl phosphine)palladium (50 mg, 0.1 mmol) was purged with argon, then anhydrous dioxane (15 mL) was added. The mixture was heated to 80°C for 24 h, quenched with aq NH_4Cl, extracted with Et_2O, washed with H_2O and brine, and dried over $MgSO_4$. Removal of solvent under reduced pressure followed by flash chromatography (silica gel, hexane/EtOAc 9:1) afforded **16** as white solid (650 mg, 88%). ^{1}H NMR (500 MHz, $CDCl_3$): $\delta=8.47$ (d, $J=2.5$ Hz, 1H), 8.02 (d, $J=7.5$ Hz, 2H), 7.74 (d, $J=8.5$ Hz, 1H), 7.54 (dd, $J=5.5$, 2.5 Hz, 1H), 7.49–7.41 (m, 3H), 1.43 ppm (s, 18H); ^{13}C NMR (125 MHz, $CDCl_3$): $\delta=156.0$, 151.2, 148.8, 138.5, 135.9, 134.7, 129.2, 128.8, 126.9, 120.0, 83.4, 27.9 ppm; MS (TOF-LD): m/z calcd for $C_{21}H_{26}N_2O_4$: 370; found: 371 $[M+H]^+$.

2-Phenyl-5-aminopyridine dihydrochloride (5): Compound **16** (371 mg, 1 mmol) and 4N HCl (3 mL) in EtOH (10 mL) gave **5** as a white solid (136 mg, 80%). ^{1}H NMR (500 MHz, D_2O/DCl): $\delta=7.93$ (d, $J=2.5$ Hz, 1H), 7.83 (d, $J=8.5$ Hz, 1H), 7.73 (dd, $J=6$, 3 Hz, 1H), 7.64–7.62 (m, 2H), 7.56–7.52 ppm (m, 3H); ^{13}C NMR (125 MHz, D_2O/DCl): $\delta=146.6$, 141.3, 131.9, 131.5, 131.4, 130.3, 127.3, 126.6, 126.3 ppm; MS (TOF-LD): m/z calcd for $C_{11}H_{10}N_2$: 170; found: 170.79 $[M+H]^+$.

Inclusion complex of 1 with 5 (5@1): Complex **5@1** was prepared by using the same procedure as described for **2@1**. ^{1}H NMR (500 MHz, D_2O/DCl): $\delta=9.17$ (d, $J=9.5$ Hz, 1H), 8.79 (s, 1H), 8.46 (d, $J=9$ Hz, 1H), 7.28 (d, $J=8$ Hz, 2H), 6.94 (t, $J=7$ Hz, 1H), 6.73 (t, $J=7.5$ Hz, 1H), 5.64 (dd, $J=61.5$, 15.5 Hz, 12H), 5.49 (s, 12H), 4.27 ppm (t, $J=16$ Hz, 12H).

2-Bromo-Boc-5-aminopyridine (17): A solution of **9** (1.73 g, 10 mmol) and Et_3N (2.1 mL, 15 mmol) in CH_2Cl_2 (50 mL) was stirred for 30 min at RT. $(Boc)_2O$ (2.6 g, 12 mmol) in CH_2Cl_2 (5 mL) was added and the mixture was stirred overnight at RT, then quenched with aq NH_4Cl and extracted with CH_2Cl_2. The organic phase was separated and washed with H_2O and brine, dried over $MgSO_4$, and the solvent was removed under reduced pressure. The residue was purified by flash chromatography (silica gel, hexane/EtOAc 8:2) to give **17** as a white solid (1.9 g, 70%). ^{1}H NMR (500 MHz, $CDCl_3$): $\delta=8.22$ (d, $J=3$ Hz, 1H), 7.87 (d, $J=6$ Hz, 1H), 7.39 (d, $J=8.5$ Hz, 1H), 6.51 (s, NH), 1.49 ppm (s, 9H); MS (TOF-ES): m/z calcd for $C_{10}H_{13}BrN_2O_2$: 272; found: 271 $[M-H]^+$.

1,4-Phenylene-bis(methylene)bis(2-bromo)-Boc-5-aminopyridine (18): NaH (60%, suspended in oil, 400 mg, 9.6 mmol) was added to a stirred solution of **17** (965 mg, 3.5 mmol) in DMF (10 mL) at 0°C, and the mix-

ture was stirred at RT for 30 min. 1,4-Bis(bromomethyl)benzene (425 g, 1.6 mmol) was added and the mixture was stirred at RT for 20 h, then quenched with aq NH_4Cl, extracted with EtOAc, washed with brine, and dried over Na_2SO_4. Removal of solvent followed by column chromatography (silica gel, hexane/EtOAc 8:2) afforded **18** as a light-yellow solid (1.72 g, 76%). ^{1}H NMR (500 MHz, $CDCl_3$): δ=8.16 (s, 2H), 7.36 (d, J=8.5 Hz, 2H), 7.30 (br s, 2H), 7.13 (s, 4H), 4.80 (s, 4H), 1.38 ppm (s, 18H); ^{13}C NMR (125 MHz, $CDCl_3$): δ=154.0, 147.8, 138.5, 138.1, 136.8, 136.2, 127.8, 127.7, 81.9, 53.1, 28.2 ppm; MS (TOF-ES): m/z calcd for $C_{28}H_{32}Br_2N_4O_4$: 648; found: 671 $[M+Na]^+$.

1,4-Phenylene-bis-methylene-bis-Boc-5-aminopyridine (19): The synthesis was performed by using **18** (648 mg, 1 mM), 2-(tributyltin)pyridine (1.1 g, 3 mmol), $[Pd(PPh_3)_4]$ (46 mg, 0.04 mmol) in toluene (15 mL) and by following the procedure used for the preparation of **13**. Column chromatography (silica gel, EtOAc/Et_3N 100:2) afforded **19** as a white solid (496 mg, 77%). ^{1}H NMR (500 MHz, $CDCl_3$): δ=8.64 (d, J=4 Hz, 2H), 8.46 (s, 2H), 8.32 (d, J=8 Hz, 2H), 8.30 (d, J=8.5 Hz, 4H), 7.78 (td, J=6, 1.5 Hz, 2H), 7.55 (d, J=7.5 Hz, 2H), 7.27 (t, J=6 Hz, 2H), 7.17 (s, 4H), 4.86 (s, 4H), 1.42 ppm (s, 18H); ^{13}C NMR (125 MHz, $CDCl_3$): δ=155.6, 154.3, 153.1, 149.1, 146.9, 139.2, 137, 136.9, 134.3, 127.8, 123.5, 121.0, 120.7, 81.4, 53.2, 28.2 ppm; MS (TOF-ES): m/z calcd for $C_{38}H_{40}N_6O_4$: 644; found: 645 $[M+H]^+$.

***N,N′*-[1,4-Phenylenebis(methylene)]di-2,2′-bipyridin-5-aminium chloride (3)**: Compound **19** (200 mg, 0.31 mmol) was dissolved in EtOH (8 mL) and 4 N HCl (3 mL) and stirred overnight at RT. The solvent was removed under reduced pressure, and the residue was dissolved in small amount of MeOH. Et_2O was added and the resultant yellowish precipitate was collected by filtration and found to be pure **3** (121 mg, 88%). ^{1}H NMR (500 MHz, D_2O/DCl): δ=8.04 (d, J=5.5 Hz, 2H), 7.83 (td, J=7.5, 1 Hz, 2H), 7.60 (d, J=3 Hz, 2H), 7.56 (s, 4H), 7.31 (t, J=6.5 Hz, 2H), 7.24 (d, J=8 Hz, 2H), 6.94 (d, J=8.5 Hz, 2H), 6.75 (dd, J=2.5, 6 Hz, 2H), 4.37 ppm (s, 4H); ^{13}C NMR (125 MHz, D_2O/DCl): δ=147.6, 147.5, 145.1, 143.2, 139.0, 134.2, 132.9, 129.6, 125.1, 124.2, 121.6, 121.4, 45.9 ppm; MS (TOF-LD): m/z calcd for $C_{28}H_{24}N_6$: 444; found: 443 $[M-H]^+$.

Inclusion complex of 1 with 3 (3@1): Complex **3@1** was prepared by using the above-described procedure for the preparation of **2@1**. ^{1}H NMR (500 MHz, D_2O/DCl): δ=8.51–6.0 (m, 14H), 5.80–5.54 (m, 24H), 5.45–5.42 (br m, 24H), 4.27–4.14 ppm (m, 28H); MS (TOF-LD): m/z calcd for $C_{100}H_{100}Cl_4N_{54}O_{24}$: 2584; found: 1257, 1258: $[M-4HCl+2K]^{2+}$.

***N*-(2,2′-Bipyridin-5-yl)-2-phenylacetamide (20)**: NaH (18 mg, 0.45 mmol, 60% in mineral oil) was added to a solution of **2** (52 mg, 0.3 mmol) in THF (5 mL), and the mixture was stirred for 30 min at RT. A solution of benzoyl chloride (52 mg, 0.33 mmol) in THF (1 mL) was added, and the mixture was stirred for 5 h at RT, then quenched with aq NH_4Cl and THF. The solvent was concentrated under reduced pressure, EtOAc was added, and the organic layer was separated. The aqueous phase was washed twice with EtOAc and the combined organic extracts were washed with brine, dried over Na_2SO_4, and concentrated under reduced pressure. Flash chromatography (silica gel, hexane/EtOAc 1:1) afforded **20** as a colorless solid (83 mg, 95%). ^{1}H NMR (500 MHz, $CDCl_3$): δ=8.64 (d, J=5 Hz, 1H), 8.58 (d, J=2.5 Hz, 1H), 8.32 (d, J=8.5 Hz, 1H), 8.29 (d, J=8 Hz, 1H), 8.14 (dd, J=6, 2.5 Hz, 1H), 7.77 (td, J=6, 2 Hz, 1H), 7.42–7.33 (m, 5H), 7.27 (ddd, J=2, 3.5, 1 Hz, 1H), 3.78 ppm (s, 2H); ^{13}C NMR (125 MHz, $CDCl_3$): δ=169.5, 155.6, 151.9, 149.1, 140.3, 136.9, 134.6, 133.9, 129.5, 129.3, 127.9, 127.6, 123.4, 121.2, 120.7, 44.7 ppm; MS (TOF-ES): m/z calcd for $C_{18}H_{15}N_3O$: 289; found: 288 $[M-H]^+$.

2-(2-Ethyl-1,3-dioxan-2-yl)ethanol (23): A mixture of **22** (2 g, 13.9 mmol), 1,3-propandiol (1.3 g, 17 mmol), and *p*-TsOH (265 mg, 1.4 mmol) in benzene (30 mL) was heated at reflux under azeotropic distillation for 20 h, then quenched with aq $NaHCO_3$ and extracted with EtOAc. The combined organic extracts were washed with $NaHCO_3$ (3×), H_2O (3×), and then with brine. The mixture was dried over $MgSO_4$, concentrated under reduced pressure, and used in the next step without further purification. $LiAlH_4$ (725 mg, 18.6 mmol) was slowly added to a solution of the above crude mixture (2.5 g, 12.4 mmol) in anhydrous Et_2O (50 mL) at 0°C under argon. The reaction mixture was heated at reflux for 5 h, then quenched by slow addition of H_2O at 0°C and filtered through Celite. The filtrate was washed with brine, dried over $MgSO_4$, and concentrated under reduced pressure. Column chromatography (silica gel, hexane/EtOAc 1:1) afforded **23** as a colorless oil (1.78 g, 78% over two steps). ^{1}H NMR (500 MHz, $CDCl_3$): δ=3.94 (td, J=11.5, 3 Hz, 2H), 3.86–3.78 (m, 4H), 3.03 (t, J=5 Hz, OH), 1.93–1.83 (m, 5H), 1.45 (dt, J=13, 3.5 Hz, 1H), 0.86 ppm (t, J=7.5 Hz, 3H); ^{13}C NMR (125 MHz, $CDCl_3$): δ=102.0, 59.3, 58.5, 38.0, 37.9, 25.2, 24.1, 7.7 ppm.

2-(2-Ethyl-1,3-dioxan-2-yl)ethyl-1*H*-imidazole-1-carboxylate (24): Carbonyldiimidazole (1.6 g, 10 mmol) was added to a stirred solution of **23** (800 mg, 5 mmol) in CH_2Cl_2 (20 mL) at 0°C and stirred for a further 2 h, then diluted with CH_2Cl_2, washed with brine, dried over $MgSO_4$, and concentrated under reduced pressure to give crude **24**, which was used for next step without further purification.

2-(2-Ethyl-1,3-dioxan-2-yl)ethyl-6-bromopyridin-3-yl carbamate (25): NaH (60% in mineral oil, 350 mg, 8.7 mmol) was slowly added to a solution of **24** (815 mg, 3.2 mmol) and **9** (500 mg, 2.9 mmol) in anhydrous THF (20 mL). The mixture was stirred overnight at RT, then quenched with aq NH_4Cl, extracted with EtOAc, washed with brine, dried over Na_2SO_4, and concentrated under reduced pressure. Column chromatography (silica gel, hexane/EtOAc 1:1) afforded **25** as a white solid (933 mg, 90% over two steps). ^{1}H NMR (500 MHz, $CDCl_3$): δ=8.28 (d, J=2.5 Hz, 1H), 7.88 (br s, 1H), 7.40 (d, J=9 Hz, 1H), 6.87 (s, NH), 4.34 (t, J=7 Hz, 2H), 3.93–3.82 (m, 4H), 2.06 (t, J=7.5 Hz, 2H), 1.83–1.72 (m, 3H), 1.57–1.53 (m, H), 0.90 ppm (t, J=7.5 Hz, 3H); ^{13}C NMR (125 MHz, $CDCl_3$): δ=153.4, 140.2, 134.9, 134.6, 128.5, 128, 99.6, 62.0, 59.4, 34.0, 25.9, 25.2, 7.6 ppm; MS (TOF-ES): m/z calcd for $C_{14}H_{19}N_2O_4Br$: 358/360 (1:1 ratio ^{79}Br/^{81}Br); found: 359/361 $[M+H]^+$.

2-(2-Ethyl-1,3-dioxan-2-yl)ethyl 2,2′-bipyridin-5-yl carbamate (26): This compound was prepared by using **25** (425 mg, 1.2 mmol), 2-(tributyltin)-pyridine (480 mg, 1.3 mmol), and $[Pd(PPh_3)_4]$ (30 mg, 0.024 mmol) in toluene (10 mL) at 120°C and by following the above-described procedure for the preparation of **13**. The crude product was purified by column chromatography (silica gel, hexane/EtOAc 1:1) to afford **26** as a yellowish solid (279 mg, 65%). ^{1}H NMR (500 MHz, $CDCl_3$): δ=8.64 (d, J=4.5 Hz, 1H), 8.56 (d, J=2 Hz, 1H), 8.35 (d, J=9 Hz, 1H), 8.32 (d, J=8 Hz, 1H), 8.07 (br d, J=6 Hz, 1H), 7.78 (t, J=8 Hz, 1H), 7.26 (t, J=6 Hz, 1H), 6.92 (s, 1H), 4.35 (t, J=7.5 Hz, 2H), 3.93–3.84 (m, 4H), 2.09 (t, J=7.5 Hz, 2H), 1.84–1.75 (m, 3H), 1.60–1.55 (m, 1H), 0.91 ppm (t, J=7.5 Hz, 1H); ^{13}C NMR (125 MHz, $CDCl_3$): δ=155.8, 153.5, 151.1, 149.1, 139.4, 136.8, 135.0, 126.2, 123.2, 121.3, 120.6, 99.6, 61.8, 59.4, 33.8, 26.1, 25.1, 7.6 ppm; MS (TOF-ES): m/z calcd for $C_{19}H_{23}N_3O_4$: 357; found: 358 $[M+H]^+$ and 356 $[M-H]^+$.

3-Oxopentyl-2,2′-bipyridin-5-yl carbamate (21): A solution of **26** (60 mg, 0.17 mmol) in AcOH/H_2O (1:9, 10 mL) was stirred overnight at RT. The mixture was quenched with aq $NaHCO_3$, extracted with CH_2Cl_2, washed with brine, dried over $MgSO_4$ and concentrated to give **21** as a white solid (48 mg, 95%). ^{1}H NMR (500 MHz, $CDCl_3$): δ=8.64 (d, J=4 Hz, 1H), 8.55 (s, 1H), 8.35 (d, J=8.5 Hz, 1H), 8.30 (d, J=8 Hz, 1H), 8.05 (br s, 1H), 7.78 (t, J=8 Hz, 1H), 7.28–7.26 (m, 1H), 6.93 (s, 1H), 4.49 (t, J=6 Hz, 1H), 2.82 (t, J=6 Hz, 1H), 2.49 (q, J=7.5, 7 Hz, 1H), 1.09 ppm (t, J=7.5 Hz, 1H); ^{13}C NMR (125 MHz, $CDCl_3$): δ=208.3, 155.7, 153.1, 151.3, 149.1, 139.4, 136.9, 134.7, 126.3, 123.3, 121.3, 120.6, 60.5, 41.2, 36.3, 7.5 ppm; MS (TOF-ES): m/z calcd for $C_{16}H_{17}N_3O_3$: 299; found: 300 $[M+H]^+$.

Acknowledgements

This study was supported by the Israel Science Foundation, the German-Israeli Project Cooperation (DIP), the Institute of Catalysis Science and Technology, Technion, and the Skaggs Institute for Chemical Biology. E.K. is the incumbent of the Benno Gitter & Ilana Ben-Ami Chair of Biotechnology, Technion. G.P. thanks the Schulich scholarship for a graduate school fellowship. A.K. was supported in part at the Technion by a fellowship from the Israel Council for Higher Education.

[1] a) W. M. Nau, G. Ghale, A. Hennig, H. Bakirci, D. Bailey, *J. Am. Chem. Soc.* **2009**, *131*, 11558; b) A. Hennig, H. Bakirci, W. M. Nau, *Nat. Methods* **2007**, *4*, 629.
[2] J. Lagona, P. Mukhopadhyay, S. Chakrabati, L. Isaacs, *Angew. Chem.* **2005**, *117*, 4922; *Angew. Chem. Int. Ed.* **2005**, *44*, 4844.
[3] a) S. Sasmal, M. K. Sinha, E. Keinan, *Org. Lett.* **2004**, *6*, 1225; b) I. Ben Shir, S. Sasmal, T. Mejuch, M. K. Sinha, M. Kapon, E. Keinan, *J. Org. Chem.* **2008**, *73*, 8772.
[4] a) W. M. Nau, J. Mohanty, *Intl. J. Photoenergy* **2005**, *7*, 133; b) B. D. Wagner, N. Stojanovic, A. I. Day, R. J. Blanch, *J. Phys. Chem. B* **2003**, *107*, 10741; c) C. Marquez, F. Huang, W. M. Nau, *IEEE Trans. Nanobiosci.* **2004**, 39; d) H.-J. Buschmann, E. Schollmeyer, *J. Inclusion Phenom. Mol. Recognit. Chem.* **1997**, *29*, 167.
[5] a) N. Saleh, A. L. Koner, W. M. Nau, *Angew. Chem.* **2008**, *120*, 5478; *Angew. Chem. Int. Ed.* **2008**, *47*, 5398; b) R. Wang, L. Yuan, D. H. Macartney, *Chem. Commun.* **2005**, 5867; c) A. Praetorius, D. M. Bailey, T. Schwarzlose, W. M. Nau, *Org. Lett.* **2008**, *10*, 4089; d) A. L. Koner, W. M. Nau, *Supramol. Chem.* **2007**, *19*, 55; e) J. Mohanty, A. C. Bhasikuttan, W. M. Nau, H. Pal, *J. Phys. Chem. B* **2006**, *110*, 5132.
[6] a) H. Cong, Y.-J. Zhao, S.-F. Xue, Z. Tao, Q.-J. Zhu, *J. Mol. Model.* **2007**, *13*, 1221; b) Z. Limei, Z, Jiannan, Z. Yunqian, Z. Qianjiang, X. Saifen, Z. Tao, Z. Jianxin, Z. Xin, W. Zhanbin, L. Lasheng, A. I. Day, *Supramol. Chem.* **2008**, 1; c) Y. Zhao, S. Xue, Q. Zhu, Z. Tao, J. Zhang, Z. Wei, L. Long, M. Hu, H. Xiao, A. I. Day, *Chin Sci. Bull.* **2004**, *49*, 1111.
[7] W. M. Nau, G. Ghale, A. Hennig, H. Bakirci, D. Bailey, *J. Am. Chem. Soc.* **2009**, *131*, 11558.
[8] a) D. Pappo, T. Mejuch, O. Reany, E. Solel, M. Gurram, E. Keinan, *Org. Lett.* **2009**, *11*, 1063; b) A. F. Littke, G. C. Fu, *Angew. Chem.* **1998**, *110*, 3586; *Angew. Chem. Int. Ed.* **1998**, *37*, 3387.
[9] S. Wu, S. Chen, M. Li, J. Xiang, Y. Xiao, L. Yuan, *Cryst. Eng.* **2007**, *10*, 907.
[10] A. Moissette, Y. Batonneau, C. Bremard, *J. Am. Chem. Soc.* **2001**, *123*, 12325.
[11] W. Rettig, R. Lapouyade in *Topics in Fluorescence Spectroscopy, Vol. 4* (Ed.: J. R. Lakowicz), Plenum Press, New York, **1994**, pp. 109–149.
[12] W. Rettig, *Angew. Chem.* **1986**, *98*, 969; *Angew. Chem. Int. Ed. Engl.* **1986**, *25*, 971.
[13] S.-S. Sun, A. J. Lees, *J. Photochem. Photobiol. A* **2001**, *140*, 157.
[14] G. Qian, M. Wang, *Mater. Lett.* **2002**, *56*, 71.
[15] *Photophysics of Aromatic Molecules* (Ed.: J. B. Birks), Wiley, New York, **1970**, p. 301.
[16] K. A. Connors, *Binding Constants: The Measurement of Molecular Complex Stability* (Ed.: K. A. Connors), Wiley, New York, **1987**, p. 27.
[17] K. A. Connors, *Binding Constants: The Measurement of Molecular Complex Stability* (Ed.: K. A. Connors), Wiley, New York, **1987**, p. 61.
[18] The overall binding constant, β, is defined as $\beta = K_1 \times K_2 \times \ldots \times K_i$ in which K_i is the binding constant of the *i*th ligand (L) to the macromolecule.
[19] P. Job, *Ann. Chim.* **1928**, *9*, 113.
[20] M. R. Eftink in *Methods in Enzymology, Vol. 278* (Eds.: L. Brand, M. L. Johnson), Academic Press, New York, **1997**, pp. 221–245.
[21] a) W. L. Mock, N. Y. Shih, *J. Org. Chem.* **1986**, *51*, 4440; b) M. V. Rekharsky, Y. H. Ko, N. Selvapalam, K. Kim, Y. Inoue, *Supramol. Chem.* **2007**, *19*, 39.
[22] *Advances in Heterocyclic Chemistry* (Eds.: A. R. Katritzky, J. M. Lagowski), Academic Press, New York, **1976**.
[23] K. D. Lay, K. S. Schanze, *Coord. Chem. Rev.* **1998**, *171*, 287.
[24] K. E. Bethin, T. R. Cimato, M. J. Ettinger, *J. Biol. Chem.* **1995**, *270*, 20703.
[25] T. Omori, R. Kimizuka, K. Yoshihara, M. Yagi, *J. Radioanal. Nucl. Chem.* **1984**, *87*, 260.
[26] M. V. Rekharsky, Y. H. Ko, N. Selvapalam, K. Kim, Y. Inoue, *Supramol. Chem.* **2007**, *19*, 39.
[27] a) W. L. Mock, *Top. Curr. Chem.* **1995**, *175*, 1; b) C. Márquez, R. R. Hudgins, W. M. Nau, *J. Am. Chem. Soc.* **2004**, *126*, 5806.
[28] J.-P. Goddard, J.-L. Reymond, *Trends Biotechnol.* **2004**, *22*, 363.
[29] A. Roa, J. L. Garcia, F. Salto, E. Cortes, *Biochem. J.* **1994**, *303*, 869.
[30] Y. Weiss, A. Shulman, I. Ben Shir, E. Keinan, S. Wolf, *Nat. Biotechnol.* **2006**, *24*, 713.
[31] H. Nierengarten, J. Rojo, E. Leize, J.-M. Lehn, A. V. Dorsselaer, *Eur. J. Org. Chem.* **2002**, 573.
[32] A. T. R. Williams, S. A. Winfield, J. N. Miller, *Analyst* **1983**, *108*, 1067.
[33] H. E. Zimmerman, J. H. Penn, C. W. Carpenter, *Proc. Natl. Acad. Sci. USA* **1982**, *79*, 2128.

Received: November 7, 2009
Revised: March 25, 2010
Published online: June 22, 2010

